Available online at www.sciencedirect.com
SCIENCE DIRECT®
Biochemical and Biophysical Research Communications 323 (2004) 112–117
BBRC
www.elsevier.com/locate/ybbrc

Redox modulation of tau and microtubule-associated protein-2 by the glutathione/glutaredoxin reductase system☆

Lisa M. Landino*, Sarah H. Robinson, Tabor E. Skreslet, Diana M. Cabral

Department of Chemistry, The College of William and Mary, P.O. Box 8795, Williamsburg, VA 23187-8795, USA

Received 10 August 2004
Available online 27 August 2004

Abstract

Alterations in the redox status of proteins have been implicated in the pathology of several neurodegenerative diseases including Alzheimer's and Parkinson's. We report that peroxynitrite and H_2O_2-induced disulfides in the porcine brain microtubule-associated proteins tau and microtubule-associated protein-2 are substrates for the glutaredoxin reductase system composed of glutathione reductase, human or *Escherichia coli* glutaredoxin, reduced glutathione, and NADPH. Oxidation and reduction of cysteines in tau and microtubule-associated protein-2 were quantitated by monitoring the incorporation of 5-iodoacetamido-fluorescein, a thiol-specific labeling reagent. Reduction of disulfide bonds in the microtubule-associated proteins by the glutaredoxin reductase system restored their ability to promote the assembly of microtubules composed of purified porcine tubulin. Thiol-disulfide exchange between oxidized glutathione and the microtubule-associated proteins was detected by monitoring protein oxidation and was quantitated by measuring reduced glutathione by HPLC.

Keywords: Peroxynitrite; Hydrogen peroxide; Microtubule-associated proteins; Tau; MAP2; Cysteine oxidation; Glutathione; Glutaredoxin; Glutathione reductase; Thiol-disulfide exchange; Disulfide bonds

Neuron-specific oxidative damage to proteins as well as cytoskeletal abnormalities have been detected in the brains of those afflicted with Alzheimer's disease [1–4]. Consequently, we are interested in studying the effects of reactive oxygen species including peroxynitrite anion ($ONOO^-$) and hydrogen peroxide (H_2O_2) on the abundant cytoskeletal protein tubulin and two neuron-specific microtubule-associated proteins (MAPs), tau and MAP2 [5,6]. Microtubules, composed of tubulin and MAPs, are essential cytoskeletal elements and are among the most abundant structures in neurons; therefore, they are likely candidates for modification by oxidants [7,8].

Recently we showed that tau and MAP2 are readily oxidized by both $ONOO^-$ and H_2O_2 to form disulfide-linked species and that the oxidized proteins are substrates for the thioredoxin reductase system (TRS) [9]. The reversible oxidation and reduction of MAPs had profound effects on the kinetics of microtubule polymerization. The fact that a repair system for oxidative damage to tau and MAP2 exists suggests that fluctuations in the redox state of neurons may regulate microtubule polymerization.

Reduced glutathione (GSH), glutaredoxin (Grx), glutathione reductase (GR), and NADPH comprise the

☆ *Abbreviations:* β-ME, β-mercaptoethanol; DTNB, dithiobis(2-nitrobenzoic acid); DTT, dithiothreitol; GR, glutathione reductase; Grx, glutaredoxin; GRS, glutathione reductase system; GSH, reduced glutathione; GSSG, oxidized glutathione; IAF, 5-iodoacetamido-fluorescein; MAPs, microtubule-associated proteins; NFTs, neurofibrillary tangles; $ONOO^-$, peroxynitrite anion; PHFs, paired helical filaments; PME buffer, 0.1 M Pipes, 1 mM $MgSO_4$, 1 mM EGTA; TCEP, tris(2-carboxyethyl)phosphine hydrochloride; Trx, thioredoxin; TrxR, thioredoxin reductase; TRS, thioredoxin reductase system.

* Corresponding author. Fax: +1 757 221 2715.
E-mail address: lmland@wm.edu (L.M. Landino).

0006-291X/$ - see front matter © 2004 Elsevier Inc. All rights reserved.
doi:10.1016/j.bbrc.2004.08.065

glutathione/glutaredoxin repair system (GRS) which is capable of reducing protein disulfides [10–12]. Grx is a small redox active protein, similar to thioredoxin that readily undergoes thiol-disulfide exchange with GSH and oxidized glutathione (GSSG) [11]. The GRS generally requires a mixed disulfide substrate between oxidized protein and GSH whereas most protein disulfides are substrates for the TRS [12].

$$P(SS) + Grx(red) \rightarrow PSH_2 + Grx(ox) \quad (1)$$

$$Grx(ox) + 2GSH \rightarrow Grx(red) + GSSG \quad (2)$$

$$GSSG + NADPH \rightarrow 2GSH + NADP^+ \quad (3)$$

In reaction (1), a protein disulfide (P(SS)) is reduced by Grx. Oxidized Grx then undergoes thiol-disulfide exchange with GSH to yield GSSG (reaction (2)) which is reduced to GSH by GR in reaction (3). NADPH oxidation supplies the energy for this repair system.

Regulation of proteins via oxidation, reduction, and/or modification of their cysteine residues by oxidants, nitric oxide or GSH is a subject of considerable research [13–15]. We detected glutathionylation of tubulin by dot blot when $ONOO^-$-damaged tubulin was incubated with GSH [16]. Given the reactivity of glutaredoxin toward mixed disulfides of protein and GSH, it is not surprising that glutathionylation of tubulin was detected; in fact, glutathionylation of β-tubulin in endothelial-like cells has been reported [17,18].

Our present study shows that disulfides in tau and MAP2 are substrates for the GRS and optimal repair requires Grx. We also provide evidence for direct thiol-disulfide exchange between the cysteines of native tau and MAP2 and GSSG to yield oxidized proteins. Based on our recent work showing that cysteines of tubulin, tau, and MAP2 are readily oxidized by $ONOO^-$ and H_2O_2, it is reasonable to suggest that microtubule polymerization could be regulated by fluctuations in the redox state of cells [9,16,19,20]. This hypothesis is reinforced by our data showing that the disulfides in tubulin, tau and MAP2 can be repaired by both the thioredoxin and glutaredoxin reductase systems.

Materials and methods

Materials

Porcine brains were obtained from Smithfield Packing Company in Smithfield, Virginia. *Escherichia coli* and human glutaredoxin were from American Diagnostica, BCA protein assay reagent and 5-iodoacetomido-fluorescein (IAF) were from Pierce. All other reagents were from either Sigma or Fisher Scientific.

Methods

Purification of brain tubulin and heat-stable MAPs. Tubulin and heat-stable MAPs were purified from porcine brain by cycles of temperature-dependent polymerization and depolymerization and phosphocellulose chromatography as described [21]. Tubulin (typically 2.5–3.5 μg/μl) in PME buffer (0.1 M Pipes, pH 6.9, 1 mM $MgSO_4$, and 2 mM EGTA) was aliquoted and stored at −80 °C. Total MAPs were eluted from the phosphocellulose column in PME buffer containing 500 mM NaCl. Heat-stable MAPs were obtained as described by Vallee [22], desalted into PME buffer, and stored at −80 °C. Tubulin and MAPs concentrations were determined by the bicinchoninic acid (BCA) protein assay (Pierce).

Synthesis of $ONOO^-$. $ONOO^-$ was synthesized from acidified H_2O_2 and sodium nitrite as described [23]. The concentration of $ONOO^-$ was determined by measuring the absorbance at 302 nm ($\varepsilon_{302} = 1670\ M^{-1}cm^{-1}$) in 0.4 M NaOH.

DTNB assay. Heat-stable porcine MAPs (1.9 μg/μl, 40 μl) were treated with 0.1 M NaOH (control), $ONOO^-$ in 0.1 M NaOH for 5 min or with H_2O_2 for 20 min at room temp. Each protein sample was treated with 35 μl of 8 M guanidine–HCl and 25 μl of 1.2 mM DTNB and absorbance values (100 μl total volume) were recorded at 412 nm within 10 min. Molar concentrations of free cysteines in the protein samples were calculated from a GSH standard curve (final concentrations from 20 to 100 μM). Absorbance values for the standards were also measured in the presence of guanidine–HCl.

Labeling of cysteines with IAF. Heat stable MAPs (1.2 μg/μl, 20 μl) were treated with 0.1 M NaOH (control), $ONOO^-$ for 2 min or H_2O_2 for 20 min at 25 °C. $ONOO^-$ stock solutions were diluted with 0.1 M NaOH immediately prior to use and the volume of $ONOO^-$ solution added to achieve the indicated concentrations was normalized (1.5 μl) to avoid variations in pH. Likewise, H_2O_2 samples were also treated with an equivalent volume of NaOH. Varying amounts of tris(2-carboxyethyl)phosphine hydrochloride (TCEP), GSH, Grx, GR, and NADPH in a final volume of 10–15 μl were then added to the samples and incubated at 25 °C for 20 min. IAF in DMF was added to final concentrations of 1.5–2.5 mM and samples were incubated at 37 °C for 30 min. Proteins were resolved by SDS–PAGE on a 7.5% gel under reducing conditions and gel images were captured using a Kodak DC290 system and a UV transilluminator. The intensity of the fluorescein-labeled protein bands was measured using Kodak 1D Image Analysis software.

Microtubule polymerization assays. Aliquots of heat stable MAPs (1.2 μg/μl, 20 μl) in PME buffer were treated with $ONOO^-$ or 0.1 M NaOH (control) at 25 °C for 5 min or with H_2O_2/NaOH for 20 min. Following treatment with the oxidants, the components of the GRS including *E. coli* or human Grx, GSH, GR, and NADPH or the disulfide reducing agent TCEP were added to the MAPs samples in a total volume of 10–15 μl. All reagents added after $ONOO^-$ were dissolved in 0.1 M phosphate buffer, pH 7.4. Following a 20 min incubation at 25 °C, the MAPs samples were combined with purified porcine tubulin (80 μl, 2.0 μg/μl) on ice and GTP was added to a final concentration of 1.25 mM. The entire sample (110–115 μl) was transferred to a 96-well plate and microtubule assembly was monitored at 340 nm for 18 min using a thermostated (37 °C) Bio-tek ELx808-UV plate reader. Following assembly, samples were transferred to microcentrifuge tubes and microtubules were collected by centrifugation at 16,000*g* for 30 min. Supernatant protein was removed following centrifugation and protein concentrations were determined by the BCA assay.

Quantitation of GSH following tubulin thiol-disulfide exchange with GSSG. Heat-stable MAPs (1.9 μg/μl, 20 μl) in PME buffer were reacted with 0–2 mM GSSG in 0.1 M phosphate buffer at pH 6.9, 7.4 or 8.0 at 37 °C for 30 min (40 μl total volume). IAF in DMF was added to a final concentration of 1.5 mM and samples were incubated at 37 °C for 30 min. Cold ethanol was added to 80% to precipitate the fluorescein-labeled MAPs and the protein was collected by centrifugation at 16,000*g* for 20 min. The supernatant containing fluorescein-labeled GSH (GS-AF) was treated with DTT to convert excess IAF to the more stable DTT adduct (DTT-AF). Samples (20 μl supernatant) were analyzed by reverse phase HPLC on a C8 column (Zorbax). Solvent A

contained 20% acetonitrile/0.1% TFA and solvent B contained 70% acetonitrile/0.1% TFA. A linear gradient from 0% to 50% B over 20 min was used to elute GS-AF (retention time = 7 min) and DTT-AF (retention time = 11 min). Fluorescein-labeled products were detected at 440 nm, the absorbance maximum of fluorescein in solvent A. GS-AF was quantitated by comparison of peak areas to a standard curve created following injection of known amounts of a GS-AF standard prepared by reacting GSH with IAF.

Results and discussion

Previously we showed that both $ONOO^-$ and H_2O_2 oxidized cysteines of the major MAPs, tau, and MAP2 [9]. Herein we used dithiobis(2-nitrobenzoic acid) (DTNB) to quantitate the oxidation of protein cysteines of heat-stable MAPs, a mixture composed primarily of the neuron-specific proteins tau and MAP2. Protein samples were treated with micromolar concentrations of $ONOO^-$ and H_2O_2. Approximate concentrations of tau and MAP2 used in these experiments are 12 and 2 μM, respectively. However, the molar concentration of cysteine target is greater because mammalian tau and MAP2 contain 1–2 and 7 cysteines, respectively [24].

Following treatment of heat-stable MAPs with $ONOO^-$ or H_2O_2, guanidine–HCl and DTNB were added to the protein samples. Guanidine–HCl denatures the proteins so that all cysteine residues are accessible to DTNB. DTNB reacts stoichiometrically with protein thiols to form the product, thionitrobenzoic acid, which absorbs strongly at 412 nm [25]. We calculated a concentration of 200 μM protein thiols in control MAPs from a standard curve prepared using GSH, guanidine–HCl, and DTNB.

Fig. 1A shows that as the concentration of oxidant, $ONOO^-$ or H_2O_2 increased the concentration of protein thiols decreased. For $ONOO^-$, it is important to note that a significant fraction of the $ONOO^-$ added to any buffered solution at neutral pH isomerizes to nitrate and all $ONOO^-$ reacts within 2 min [26]. In the case of H_2O_2, protein samples were treated for 20 min prior to the addition of guanidine–HCl and DTNB. At all concentrations tested, $ONOO^-$ was more effective at oxidizing protein thiols than H_2O_2 which is consistent with previous work from our laboratory and from others [9,19,27].

In addition, oxidation of protein thiols was monitored using 5-iodoacetamido-fluorescein (IAF), a thiol-specific fluorescein labeling reagent. Oxidized cysteines, whether disulfides or higher oxidation states of sulfur, cannot be labeled; thus, as the concentration of $ONOO^-$ increases, the incorporation of fluorescein into tau and MAP2 decreases. Fig. 1B shows a decrease in IAF labeling of both tau and MAP2 for those samples treated with oxidants (lanes 2 and 4). Multiple tau isoforms derived from a single gene can be seen in the region marked "tau" in Fig. 1B [28]. Likewise, the band

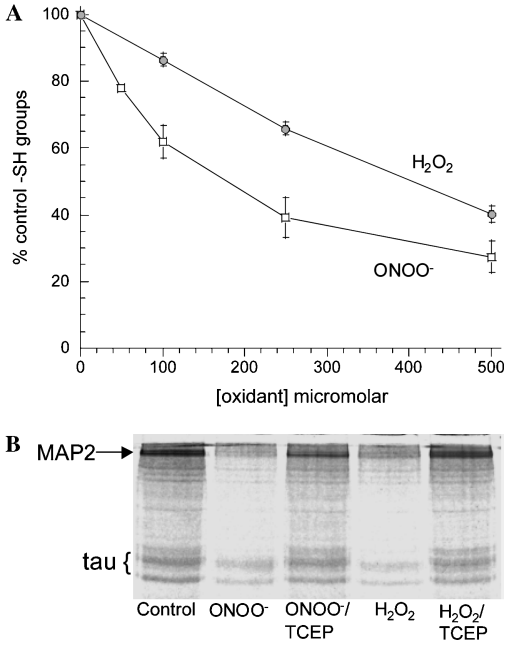

Fig. 1. Oxidation of tau and MAP2 cysteines. (A) DTNB assay. Heat-stable porcine MAPs (1.9 μg/μl, 40 μl) were treated with 0.1 M NaOH (control), $ONOO^-$ in 0.1 M NaOH for 5 min or H_2O_2 for 20 min at room temperature. Following the addition of guanidine–HCl and DTNB, absorbance values (100 μl total volume) were recorded at 412 nm. (B) Sulfhydryl-specific fluorescein labeling of tau and MAP2. Heat-stable porcine MAPs (1.2 μg/μl, 20 μl) were treated with 0.1 M NaOH (control), $ONOO^-$ for 5 min or H_2O_2 for 20 min at room temp followed by 2.5 mM TCEP or 0.1 M phosphate buffer, pH 7.4, for 20 min. Subsequently, all samples were treated with 1.5 mM IAF for 30 min at 37 °C. IAF labeling was terminated by the addition of SDS gel loading buffer containing βME. Proteins were resolved by SDS–PAGE on 7.5% gels under reducing conditions, gel images were digitized, and band intensities were measured using Kodak 1D Image Analysis software. Lane 1, control MAPs; lanes 2, 0.5 mM $ONOO^-$; lane 3, 0.5 mM $ONOO^-$ and TCEP; lane 4, 0.5 mM H_2O_2; and lane 5, 0.5 mM H_2O_2 and TCEP.

marked "MAP2" refers to two high molecular weight isoforms: MAP2A and MAP2B [24]. MAPs cysteine oxidation by 500 μM $ONOO^-$ was slightly greater than for the 500 μM H_2O_2 sample (lane 4) consistent with the DTNB results in Fig. 1A.

We also treated MAPs first with $ONOO^-$ or H_2O_2, then with TCEP, a phosphine-based disulfide reducing agent, and finally with IAF. Because TCEP is not a sulfhydryl-containing compound like βME or dithiothreitol (DTT), its presence does not affect the IAF labeling step. Fig. 1B shows that treatment of oxidant damaged MAPs with TCEP fully restores IAF labeling to control levels; tau and MAP2 band intensities in lane 1 (control MAPs) are equal to those in lane 3 ($ONOO^-$/TCEP) and lane 5 (H_2O_2/TCEP). This observation is consistent with disulfide bonds as the only type of cysteine oxidation induced by the oxidants.

The observation that disulfides were formed by oxidant treatment of MAPs, coupled with our recent work

showing that the TRS could repair oxidized MAPs, led us to ask if oxidized tau and MAP2 were substrates for the GRS [9]. Fig. 2 shows the results of the GRS repair assay after SDS–PAGE separation of the fluorescein-labeled MAPs proteins. As expected, fluorescein labeling of both tau and MAP2 is reduced following the addition of 0.5 mM $ONOO^-$ relative to control MAPs (Fig. 2, lanes 1 and 2). Treatment of $ONOO^-$ damaged MAPs with TCEP restored thiol groups that were then labeled by IAF (lane 3). Treatment of $ONOO^-$ damaged MAPs with the complete GRS (Fig. 2, lane 4) restored fluorescein labeling of tau and MAP2 to 90% and 92%, respectively, of control whereas TCEP restores labeling of both to 94–97% of control. Repair of tau and MAP2 was only barely detectable for the GRS in the absence of Grx, the intermediary protein shown in Eqs. (1) and (2). Because some repair occurred without Grx, oxidized MAPs (P(SS)) must undergo thiol-disulfide exchange with GSH according to Eq. (4).

$$P(SS) + 2GSH \rightarrow PSH_2 + GSSG \quad (4)$$

Equimolar concentrations of human and *E. coli* Grx were compared in repair assays and identical results were obtained (data not shown).

Our recently published work on MAPs oxidation and reduction by the TRS showed that cysteine oxidation had a profound effect on the ability of MAPs to promote the assembly of microtubules from purified porcine tubulin. Fig. 3 shows overlays of microtubule polymerization curves in which MAPs were pre-treated with oxidants, repaired by the GRS, and then combined with purified tubulin.

A comparison of control MAPs with $ONOO^-$-treated MAPs shows a very distinct difference in the kinetics

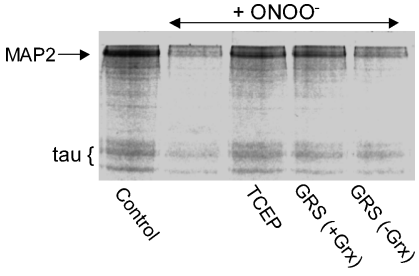

Fig. 2. Repair of tau and MAP2 cysteines by the GRS. Heat stable MAPs (1.2 μg/μl, 20 μl) were treated with 0.1 M NaOH (control) or $ONOO^-$ for 5 min at 25 °C. After a 20 min treatment with either TCEP or varying components of the GRS at 25 °C, IAF was added (2.5 mM) and samples were incubated for an additional 30 min at 37 °C. MAPs were resolved by SDS–PAGE on a 7.5% gel under reducing conditions, gel images were digitized, and band intensities were measured using Kodak 1D Image Analysis software. Lane 1, control MAPs; lane 2, MAPs treated with 0.5 mM $ONOO^-$; lane 3, oxidized tubulin treated with 2 mM TCEP; and lane 4, oxidized MAPs treated with 7 μM *E. coli* Grx, 1 mM GSH, 0.5 mM NADPH, and 0.05 U GR. Lane 5, oxidized MAPs treated with 1 mM GSH, 0.5 mM NADPH, and 0.05 U GR.

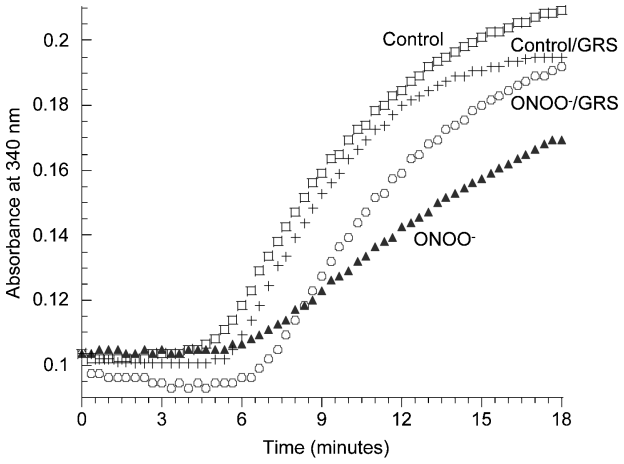

Fig. 3. Effect of MAPs oxidation and reduction on microtubule polymerization MAPs (1.2 μg/μl, 20 μl) were treated with 0.1 M NaOH (control, open square), 0.5 mM $ONOO^-$ (closed triangle), 0.1 M NaOH (control) and the complete GRS (+) or 0.5 mM $ONOO^-$/GRS (open circle), as described in Materials and methods. Following oxidation and repair, MAPs were combined with purified porcine brain tubulin (80 μl, 2.0 μg/μl) and GTP (1.25 mM). Microtubule polymerization was monitored at 340 nm in a 96-well plate thermostated to 37 °C. These results are representative of two independent experiments.

of microtubule polymerization. An extended lag phase is observed for $ONOO^-$-treated MAPs and the maximal rate of polymerization is also reduced by oxidant treatment. Because $ONOO^-$ decomposes completely within 2 min at neutral pH and oxidant-treated MAPs were prepared in a reaction separate from tubulin, the observed lag phase cannot be attributed to direct $ONOO^-$ oxidation of tubulin [19].

For those MAPs samples treated with the GRS, a complication arose because NADPH, which is part of the repair system, also absorbs at 340 nm, the wavelength used to monitor microtubule formation by light scattering. For this reason, the GRS-repaired MAPs polymerization sample does not show the same kinetics as control MAPs or even GRS-treated control MAPs. Oxidized MAPs samples were treated with the GRS for 20 min; however, repair is not 100% complete (see Fig. 2) and there is an initial decrease in absorbance for that sample in Fig. 3 because NADPH is oxidized because repair continues. Also, as the rate of polymerization reaches its maximum between 6 and 12 min, oxidation of NADPH may continue. Regardless of these experimental limitations, oxidant-treated, GRS-repaired MAPs promote microtubule assembly far better than oxidized MAPs.

Both $ONOO^-$ and H_2O_2 induce the same change in assembly kinetics and the effect is reversed by small molecule reductants, DTT and TCEP, as well as by the GRS and TRS, endogenous reductases [9]. Thus, cysteine oxidation of MAPs to disulfide species is responsible for the kinetic changes. Although $ONOO^-$ can damage several

amino acids in proteins, H_2O_2 can only oxidize cysteines and perhaps methionine [29]. Although tyrosine nitration of tau has been reported in AD brain, our work with H_2O_2 shows that tyrosine nitration of MAPs cannot be responsible for the change in polymerization kinetics that we observe [30].

GSH serves as the primary physiologic redox regulator in vivo. GSH can be oxidized by $ONOO^-$ and other cellular oxidants to its disulfide form, GSSG, and is reduced back to GSH by the NADPH-dependent enzyme, glutathione reductase [31]. GSH concentrations in most eukaryotic cells are in the 1–10 mM with a typical GSH:GSSG ratio of 100–400 [32]. Under normal physiologic conditions, GSH will protect proteins from oxidation by reactive oxygen species (ROS). However, under conditions of oxidative stress, it is hypothesized that the ratio of GSH:GSSG may decrease to as low as 1–10 and thus GSH will not be present in sufficient quantities to prevent oxidative damage to proteins. Furthermore, GSSG has been reported to undergo thiol/disulfide exchange with proteins containing reduced cysteines [32]. Thus, protein oxidation is likely when GSSG concentrations increase during oxidative stress.

Direct thiol-disulfide exchange between oxidized MAPs and GSH must occur when the GRS, in the absence of Grx, repairs oxidized tubulin (see Fig. 2, lanes 2 vs. 5). Thus, transiently high concentrations of GSSG have the potential to undergo thiol-disulfide exchange with protein thiols according to Eq. (5) which is the reverse of Eq. (4).

$$P(SH)_2 + GSSG \rightarrow P(SS) + 2GSH \quad (5)$$

To study thiol-disulfide exchange, heat-stable MAPs were treated with increasing concentrations of GSSG at pH 6.9, 7.4 or 8.0. As shown in Fig. 4A, increased protein cysteine oxidation as determined by IAF labeling was observed as the concentration of GSSG increased. As expected, the extent of protein oxidation was greatest at pH 8.0 which is consistent with attack of protein thiolates on the disulfide bond of GSSG [32]. Just below the dye front in Fig. 4A, one can see the adduct formed when GSH produced in the exchange reaction reacts with IAF. This product, GS-AF, was quantitated by HPLC to determine the extent of the exchange reaction (Fig. 4B).

We measured the concentration of GSH produced as a function of GSSG concentration at pH 7.4 and 8.0. Each protein disulfide formed yields two molecules of GSH (Eq. (5)). Fig. 4B shows the concentration dependence of GSH production by the reaction of MAPs with GSSG. The results, showing higher GSH yields at pH 8.0, are consistent with the IAF labeling experiment in Fig. 4A. For example, the reaction of 2 mM GSSG with 1 mg/ml MAPs for 30 min yielded 53 μM GSH and thus, 26.5 μM protein disulfide at pH 8.0.

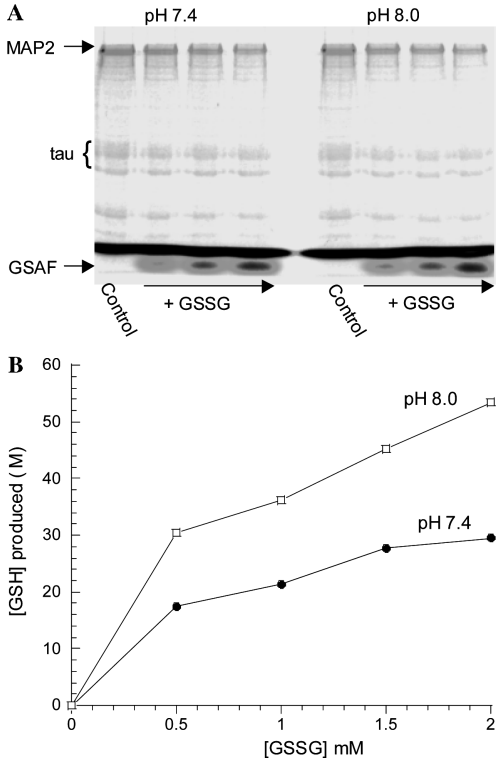

Fig. 4. Thiol-disulfide exchange between heat-stable MAPs and GSSG. (A) MAPs (1.9 μg/μl, 10 μl) were incubated with increasing concentrations of GSSG (total reaction volume = 20 μl) in 0.1 M phosphate buffer for 30 min at 37 °C. Lanes 1–4, control, 0.5, 1, and 2 mM GSSG at pH 7.4; lanes 5–8, control, 0.5, 1, and 2 mM GSSG at pH 8.0. Subsequently, all samples were treated with 1.5 mM IAF for 30 min at 37 °C. Proteins were resolved by SDS–PAGE on 7.5% gels under reducing conditions, gel images were digitized, and band intensities were measured using Kodak 1D Image Analysis software. (B) MAPs (1.9 μg/μl, 20 μl) were incubated with increasing concentrations of GSSG in 0.1 M phosphate buffer at either pH 7.4 or 8.0 for 30 min at 37 °C (40 μl total volume). GSH was converted to GS-AF by reaction with 1.5 mM IAF for 30 min at 37 °C. The GS-AF adduct was detected by reversed phase HPLC as described in Materials and methods. These data represent the average of two independent experiments performed in duplicate.

Native MAPs were also incubated with millimolar concentrations of cystine, the oxidized disulfide form of the amino acid cysteine. At all pH values tested, 6.9, 7.4, and 8.0, MAPs cysteines were oxidized in a dose-dependent manner with the greatest oxidation at pH 8.0.

Although the GGSG concentrations used in these experiments were relatively high, they were required to demonstrate the reactivity of MAPs thiols with GSSG. This work is the first to report the reaction of MAPs thiols and disulfides with GSH/GSSG and the glutaredoxin reductase system. Ultimately, we will use the reaction with GSH and GSSG to estimate redox potentials for protein thiols [32].

The results presented herein provide further support that oxidation of MAP2 and tau cysteines to disulfides

correlates with alterations in microtubule polymerization kinetics. We have determined that MAPs disulfides are substrates for both the GRS and the TRS, ubiquitous reductase systems. MAPs cysteines may be oxidized to disulfides and then rapidly reduced by either repair system. In this manner, shifts in the redox status of a neuron may modulate microtubule polymerization.

Acknowledgments

The authors acknowledge support from the National Institute of Neurological Disorders and Stroke (R15-NS38885 to L.M.L.) and the Jeffress Memorial Trust (Grant # J-670 to L.M.L).

References

[1] M.A. Smith, P.L. Richey Harris, L.M. Sayre, J.S. Beckman, G. Perry, Widespread peroxynitrite-mediated damage in Alzheimer's disease, J. Neurosci. 17 (1997) 2653–2657.
[2] M.Y. Aksenov, M.V. Aksenova, D.A. Butterfield, J.W. Geddes, W.R. Markesbery, Protein oxidation in the brain in Alzheimer's disease, Neuroscience 103 (2001) 373–383.
[3] A.D. Cash, G. Aliev, S.L. Seidlak, A. Nunomura, H. Fujioka, X. Zhu, M. Tabaton, A.B. Johnson, M. Paula-Barbosa, J. Avila, P.K. Jones, R.J. Castellani, M.A. Smith, G. Perry, Microtubule reduction in Alzheimer's disease and aging is independent of tau filament formation, Am. J. Pathol. 162 (2003) 1623–1627.
[4] M.P. Mattson, Pathways towards and away from Alzheimer's disease, Nature 430 (2004) 631–639.
[5] M.L. Garcia, D.W. Cleveland, Going new places using an old MAP: tau, microtubules and human neurodegenerative disease, Curr. Opin. Cell Biol. 13 (2001) 41–48.
[6] Y. Miyata, M. Hoshi, E. Nishida, Binding of MAP2 and tau to the intermediate filament reassembled from neurofilament 70 kDa subunit protein, J. Biol. Chem. 261 (1986) 13026–13030.
[7] S. Brady, M. Black, Axonal transport of microtubule protein: cytotypic variation of tubulin and MAPs in neurons, Ann. N. Y. Acad. Sci. 466 (1986) 199–217.
[8] B.J. Schnapp, R.D. Vale, M.P. Sheetz, T.S. Reese, Single microtubules from squid axoplasm support bidirectional movement of organelles, Cell 40 (1985) 455–462.
[9] L.M. Landino, T.E. Skreslet, J.A. Alston, Cysteine oxidation of tau and microtubule-associated protein-2 by peroxynitrite: modulation of microtubule assembly kinetics by the thioredoxin reductase system, J. Biol. Chem. 279 (2004) 35101–35105.
[10] M. Luthman, A. Holmgren, Glutaredoxin from calf thymus, J. Biol. Chem. 257 (1982) 6686–6690.
[11] A. Holmgren, F. Aslund, Glutaredoxin, Methods Enzymol. 252 (1995) 283–292.
[12] C. Johansson, C.H. Lillig, A. Holmgren, Human mitochondrial glutaredoxin reduces S-glutathionylated proteins with high affinity accepting electrons from either glutathione or thioredoxin reductase, J. Biol. Chem. 279 (2004) 7537–7543.
[13] P.J. Hogg, Disulfide bonds as switches for protein function, Trends Biochem. Sci. 28 (2003) 210–214.
[14] D.T. Hess, A. Matsumoto, R. Nudelman, J.S. Stamler, S-nitrosylation: spectrum and specificity, Nat. Cell. Biol. 3 (2001) E1–E3.
[15] S.A. Lipton, Y.-B. Choi, H. Takahashi, D. Zhang, W. Li, A. Godzik, L.A. Bankston, Cysteine regulation of protein function as exemplified by NMDA-receptor modulation, Trends Neurosci. 25 (2002) 474–480.
[16] L.M. Landino, K.L. Moynihan, J.V. Todd, K.L. Kennett, Modulation of the redox state of tubulin by the glutathione/glutaredoxin reductase system, Biochem. Biophys. Res. Commun. 314 (2004) 555–560.
[17] C. Lind, R. Gerdes, Y. Hamnell, Shuppe-Koistinen, H. Brockenhuus von Lowenhielm, A. Holmgren, I.A. Cotgreave, Identification of S-glutathionylated cellular proteins during oxidative stress and constitutive metabolism by affinity purification and proteomic analysis, Arch. Biochem. Biophys. 406 (2002) 229–240.
[18] D.W. Starke, P.B. Chock, J.J. Mieyal, Glutathione-thioyl radical scavenging and transferase properties of human glutaredoxin (thioltransferase), J. Biol. Chem. 278 (2003) 14607–14613.
[19] L.M. Landino, R. Hasan, A. McGaw, S. Cooley, A.W. Smith, K. Masselam, G. Kim, Peroxynitrite oxidation of tubulin sulfhydryls inhibits microtubule polymerization, Arch. Biochem. Biophys. 398 (2002) 213–220.
[20] L.M. Landino, J.S. Iwig, K.L. Kennett, K.L. Moynihan, Repair of peroxynitrite damage to tubulin by the thioredoxin reductase system, Free Radic. Biol. Med. 36 (2004) 497–506.
[21] R.C. Williams, J.C. Lee, Preparation of tubulin from brain, Methods Enzymol. 85 (1982) 376–385.
[22] R.B. Vallee, Reversible assembly purification of microtubules without assembly-promoting agents and further purification of tubulin, microtubule-associated proteins, and MAP fragments, Methods Enzymol. 134 (1986) 89–104.
[23] J.S. Beckman, J. Chen, H. Ischiropoulos, J.P. Crow, Oxidative chemistry of peroxynitrite, Methods Enzymol. 233 (1994) 229–240.
[24] S.A. Lewis, D. Wang, N. Cowan, Microtubule-associated protein MAP2 shares a microtubule binding motif with tau protein, Science 242 (1988) 936–939.
[25] P.W. Riddles, R.L. Blakeley, B. Zerner, Ellman's reagent: 5,5′-dithiobis(2-nitrobenzoic acid)-a reexamination, Anal. Biochem. 94 (1979) 75–81.
[26] J.S. Beckman, Oxidative damage and tyrosine nitration from peroxynitrite, Chem. Res. Toxicol. 9 (1996) 836–844.
[27] R. Radi, J.S. Beckman, K.M. Bush, B.A. Freeman, Peroxynitrite oxidation of sulfhydryls, J. Biol. Chem. 266 (1991) 4244–4250.
[28] D.W. Cleveland, S.Y. Hwo, M.W. Kirschner, Physical and chemical properties of purified tau factor and the role of tau in microtubule assembly, J. Mol. Biol. 116 (1977) 227–247.
[29] R. Radi, Kinetic analysis of reactivity of peroxynitrite with biomolecules, Methods Enzymol. 269 (1996) 354–366.
[30] T. Horiguchi, K. Uryu, H. Ischiropoulos, R. Lightfoot, C. Bellmann, C. Richter-Landsberg, V.M.-Y. Lee, J.Q. Trojanowski, Nitration of tau protein is linked to neurodegeneration in tauopathies, Am. J. Pathol. 163 (2003) 1021–1031.
[31] R. Dringen, J.M. Gutterer, Glutathione reductase from bovine brain, Methods Enzymol. 348 (2002) 281–288.
[32] H.F. Gilbert, Thiol/disulfide exchange equilibria and disulfide bond stability, Methods Enzymol. 251 (1995) 8–28.